NJC

Accepted Manuscript

This is an *Accepted Manuscript*, which has been through the Royal Society of Chemistry peer review process and has been accepted for publication.

Accepted Manuscripts are published online shortly after acceptance, before technical editing, formatting and proof reading. Using this free service, authors can make their results available to the community, in citable form, before we publish the edited article. We will replace this *Accepted Manuscript* with the edited and formatted *Advance Article* as soon as it is available.

You can find more information about *Accepted Manuscripts* in the Information for Authors.

Please note that technical editing may introduce minor changes to the text and/or graphics, which may alter content. The journal's standard Terms & Conditions and the Ethical guidelines still apply. In no event shall the Royal Society of Chemistry be held responsible for any errors or omissions in this *Accepted Manuscript* or any consequences arising from the use of any information it contains.

ROYAL SOCIETY OF CHEMISTRY

www.rsc.org/njc

Cite this: DOI: 10.1039/c0xx00000x

www.rsc.org/xxxxxx

ARTICLE TYPE

Toward white electroluminescence by ruthenium quinoxaline light emitting diodes

Hashem Shahroosvand[a]*, Shiva Rezaei[a], Ezeddin Mohajerani[b], Malek Mahmoudi[b]

[a]Chemistry Department, University of Zanjan, Zanjan, Iran.
[b]Laser and Plasma Research Institute, Shahid Beheshti University, Tehran, Iran.

Received (in XXX, XXX) XthXXXXXXXXX 20XX, Accepted Xth XXXXXXXXX 20XX
DOI: 10.1039/b000000x

Ancillary ligand substitution in the new series $[Ru(dicnq)(pyTz)(X)]^+$ {dicnq=6,7-dicyanodipyrido[2,2-d:2′,3′-f]quinoxaline and X=2, 2-bipyridine (bpy), 1,10-phenanthroline (phen), 2- pyridine tetrazole (pyTz)}, proves to be an effective way to create white electroluminescence with the Commission Internationale d'Eclairage Chromaticity Coordinates x=0.40 and y=0.39. These complexes were characterized by UV-visible and FT-IR spectroscopy, ^{1}H-NMR, CHN and Mass spectroscopy analysis. The absorption and emission spectra are consistent with low-lying MLCT excited states, which are typical of Ru(II) polypyridyl complexes. All the complexes exhibit reversible metal-centered oxidation processes undergo a one-electron oxidation within the potential range +1.30 vs SCE. On reduction, each compound undergoes several reversible or quasi reversible ligand-centered reductions (-1.65-2.40 V). It was found that white light emission can be obtained from the device ITO/PEDOT:PSS /PVK/ ruthenium complex / PBD/Al by combining Forster emission from Ru(dicnq) and Exciplex emission at PVK/Ru(dicnq) interface, although the CIE chromaticity coordinates gradually change with applied voltages. The highest luminous efficiency and luminance and lowest turn-on voltage values are obtained from the 8 wt.% Ru(dicnq)(pyTz)(bpy) doped device as 1.78 cd/A and 1030 cd /m^2 at 16 V and 5.2 V, respectively. As an important result, the incorporation of pyTz as ancillary ligand to [Ru(dicnq] complexes was found to be the most beneficial ancillary substitution in terms of creating the white electroluminescence in ruthenium quinoxaline complexes.

1. Introduction:

The emitting properties of ruthenium polypyridyl compounds have recently been successfully applied in the development of electroluminescent devices [1]. One of the reasons that ruthenium polypyridyl compounds has expanded so enormously is that compounds of this type have intriguing ground- and excited-state photophysical, photochemical and redox properties [2].

Chemical design of organic ligands in light emitting organometallic complexes can represent a powerful tool to develop full color light emitting diodes as well as to get white light, thus opening the way to lighting sources with high efficiency and low costs in alternative to inorganic LEDs, fluorescent and incandescent bulbs [3]. Two general strategies can be implemented in order to create electroluminescence in ruthenium polypyridyl complexes: (a) via molecular design, and (b) via energy transfer [4]. The synthesis method has the advantage of a fine control of the electronic structure of compounds and design of a large number of emitters with desired properties [5, 6] (For more details, please see ESI†, S1) is better. In this regard, color tuning to achieve blue, green, and red is very important because mixing of these colors can produce all colors, especially white, which is crucial for full color display applications [7]. Optimistic expectations predict that white OLED efficiencies will rapidly increase in the next ten years, reaching values similar to those expected for inorganic LEDs [8]. However, the demonstration of multiple colors of Ru polypyridyl complexes has not received much attention so far, despite the fact that red, green and blue are required for applications in lighting and full color display [9].

In particular, new ruthenium complexes with different π-conjugated ligands such as dipyrido quinoxaline derivates may overcome these drawbacks [10]. In this regard, dicnq = 6,7-dipyrido [2,2-d:2′,3′-f] quinoxaline complexes of ruthenium (II) were evaluated as potential for luminescence material [11]. In addition, among a great number of 1,10-phenanthroline derivates, dicnq as rigid π-conjugated systems is ideal candidate for DNA binding because they prevent the bending along and/or rotation around the σ-skeleton of the molecule [12] (For more samples, please see ESI, S2). Within this context, 2-pyridylazoles are also capable of using two adjacent nitrogen atoms to form a stable chelate interaction. The strong σ-donor property of the azolate, together with the π-accepting ability of the second pyridyl fragment, [13] may provide a synergism of the electron delocalization so that the electron density is transferred from azolate to the metal ion and back to the pyridyl side of the ligand, thus enhancing the chelate interaction. Exciplex formation at the interface of organic emitting layer and hole transport layer became a major subject because it changed emitting color [14]. Even though many research groups studied single layer and multilayer devices, the emission from Exciplex formation in

ruthenium polypyridyl complexes has not been completely introduced as an emitting source [15].

A specific motivation behind this study is as follows: despite the large number of red electroluminescence emission reported in ruthenium polypyridyl complexes in the literatures; their white electroluminescent properties remain unexplored [16]. Beside, the attraction of this important class of polypyridyl complexes in biological applications hustles all researchers to more depth in photonic and optoelectronic applications. Despite these attractive features, the development of dicnq and tetrazole compounds is primarily focused on the biological aspects, and has, until now, been limited. Thus, we found that the incorporation of these attractive ligands (dicnq and pyTz) into one emitting hybrid structure might provide some suggestions to create the electroluminescence-in LED devices.

This paper systematically introduces several approaches to design emitters based on Ru (dicnq)(pyTz)(X) (X=phen, bpy and pyTz), not only indicating the electroluminescence in ruthenium quinoxaline compounds but also creating white electroluminescence in this interesting class.

2. Experimental:

2.1 Materials and Instruments

All chemicals and solvents were purchased from Merck & Aldrich and used without further purification. IR spectra were recorded on a Perkin-Elmer 597 spectrometer ^{1}H-NMR spectra were recorded by use of a Bruker 400 MHz, spectrometer.. Elemental analysis was performed on Elementar Vario EL CHN elemental analyzer. Mass spectrometry was performed with a Bruker BIFLEX III mass spectrometer. Electrochemical measurements were made in DMF using model SAMA500 potentiostat. A conventional three-electrode configuration consisting of a Pt-disk working electrode and a Pt-wire auxiliary electrode. The potentials are referenced to a saturated Ag/AgCl reference electrode. In cyclic voltammetry (CV) the following parameters and relation were used: scan rate, 100 mV s^{-1}; formal potential $Eo' = (E_{pa} + E_{pc}) / 2$ where E_{pa} and E_{pc} are anodic and cathodic peak potentials, respectively; ΔE_p is the peak to-peak separation.

The supporting electrolyte was 0.1 M $[Bu_4N]BF_4$. Ferrocene was added as an internal standard after each set of measurements, and all potentials reported were quoted with reference to the ferrocene- ferrocenium (Fc/Fc^+) couple at a scan rate of 100 mV/s. The oxidation (E_{ox}) and reduction (E_{red}) potentials were used to determine the HOMO and LUMO energy levels using the equations $E_{HOMO} = -(E_{ox} + 4.8)$ eV and $E_{LUMO} = -(E_{red} + 4.8)$ eV which were calculated using the internal standard ferrocene value of -4.8 eV with respect to the vacuum [17]. The PL spectra were recorded by Avantes spectrometer Avaspec125 during 405 nm irradiation. The photoluminescence quantum yields (PLQYs) were also performed in DMF solvent. Also, $Ru(bpy)_3$ is used as reference standard for PLQYs determination [18].

The molecular and electronic structure calculations were performed with density functional theory (DFT) using the Gaussian 03(G03) program package. The B3LYP functional [19] with the LANL2DZ basis set was carried out. All geometry optimizations were performed in either C1 or C2 symmetry with subsequent frequency analysis to show that the structures are at the local minima on the potential energy surface. The electronic orbitals were visualized using GaussView 3.0.

2. 2. Synthesis of ligands and complexes

Dicnq and pyTz ligands were prepared according to the literature methods [20, 21].

Synthesis of 6,7-Dicyanodipyrido[2,2-d:2',3'-f] quinoxaline (dicnq). The *dicnq* ligand was synthesized by following the reported procedures with some changes, phendione (210mg, 1mmol) and diaminomaleonitrile (162 mg, 1.5 mmol) were dissolved in ethanol, and the resulting solution was refluxed for 1h under nitrogen atmosphere. The reaction mixture was cooled to room temperature, concentrated, and kept in an ice bath. Brownish-yellow needles were formed, which were filtered, washed with cold ethanol, and dried in vacuum.

Yield: 80%. m. p. >250 °C. Anal. Found: C, 67.98; H, 2.19; N, 29.37. Calcd. for C16H6N6: C, 68.08; H, 2.14; N, 29.57. FAB-MS: m/z 283 (M^+).;1 H NMR (DMSO-d6, 400 MHz, TMS): 9.37 (m, 4H), 7.98 (q, 2H).

Synthesis of 2- pyridine (1H-tetrazole-5-yl) (pyTz). The pyTz was prepared according to the literature method with some changes. A mixture of 2-cyano pyridine (2.05 ml, 20 mmol), 40 ml of water, sodium azide (1.43 g, 22 mmol), and 4.5 g. (20 mmol) zinc bromide were placed in round-bottomed flask with three vertical necks. The reaction was refluxed in a hood, but open to the atmosphere, for 24 hours with vigorous stirring. After the mixture was cooled to room temperature, HCl (3 N, 30 mL) and ethyl acetate (100 mL) were added, and vigorous stirring was continued until no solid was present and the aqueous layer had a pH of 1. The combined organic layers were evaporated, 200 mL of 0.25 N NaOH was added, and the mixture was stirred for 1 hour, until the original precipitate was dissolved and a suspension of zinc hydroxide was formed. The suspension was filtered, and the solid washed with 20 mL of 1 N NaOH. To the filtrate was added 40 mL of 3 N HCl with vigorous stirring causing the tetrazole to precipitate. The tetrazole was filtered and washed with 2 × 20 mL of 3 N HCl and dried in a drying oven to furnish the (pyTz) as a white or slightly colored powder.

Synthesis of [Ru(dicnq)(pyTz)(phen)]BF_4. A mixture of $RuCl_3$ (0.1g, 1mmol) and pyTz (0.07g, 1mmol) dissolved in 50 ml methanol was stirred at reflux temperature for 2h under a nitrogen atmosphere. To this solution, dicnq (0.13, 1mmol) and phen (0.1, 1mmol) were add, respectively, and the solution was heated to reflux for 3h. After cooling down to room temperature, the solution was concentrated with a rotary evaporator followed by addition of aqueous $NaBF_4$ saturated solution. The dark precipitate was filtered and washed with cold water and methanol. This product was future purified by column chromatography using alumina as column support and acetonitrile/ methanol (2: 1, v/v) as the eluent. The major black band was collected and corresponds to the desired complex. Yield: 40%. m. p. >250 °C. Anal. Found: C, 51.532; H, 2.319; N, 22.011. Calcd. for RuC34H11N18: C, 51.543; H, 2.308; N, 22.034. ESI-MS: m/z 709.741, [M-BF_4], IR (KBr, cm^{-1}): $\upsilon(C=N)_{pyTz}$ 1456, $\upsilon(N=N)_{pyTz}$ 1368, $\upsilon(C=N)_{py}$ 1625, $\upsilon(C\equiv N)_{dicnq}$=2230. ^{1}H NMR (DMSO-d6, 250 MHz): δ,9.76 (dd, 2H), 9.52 (d, 1H), 9.32 (d, 1H), 9.07 (dd, 2H), 8.92 (t, 2H), 8.72 (dd, 1H), 8.53 (d, 1H), 8.39 (dd, 2H), 8.21 (m, 2H), 7.92 (d, 1H), 7.73 (d,1H), 7.57 (dd, 1H).

Synthesis of [Ru(dicnq)(pyTz)(bpy)]BF_4. [Ru(dicnq)(pyTz)(bpy)]BF_4 was prepared starting from $RuCl_3.xH_2O$ (0.1g, 1 mmol), pyTz (0.07 g, 1 mmol), dicnq (0.13 g, 1mmol) and bpy (0.09g, 1mmol) using the same procedure as described for [Ru(dicnq)(pyTz)(phen)]BF_4 to yield the product. Yield: 44.5%. m. p. >250 °C. Anal. Found: C, 49.127; H, 2.564; N,23.749. Calcd. for RuC32H8N11: C, 49.131; H, 2.579; N, 23.733. ESI-MS:m/z 687.545, [M-BF_4], IR (KBr, cm^{-1}): $\upsilon(C=N)_{pyTz}$ 1451, $\upsilon(N=N)_{pyTz}$ 1373, $\upsilon(C=N)_{py}$ 1620, $\upsilon(C\equiv N)_{dicnq}$=2218. ^{1}H NMR (DMSO-d6, 250 MHz): δ,9.65 (dd,

2H), 9.42 (dd, 2H), 9.37 (dd, 2H), 8.88 (d, 1H), 8. 72 (d, 1H), 8.52 (m, 4H), 8.34 (dd, 1H), 8.15 (dd, 1H), 7.82 (dd, 2H), 7.61 (dd, 1H), 7.49 (t, 1H).

Synthesis of [Ru(dicnq)(pyTz)$_2$]. This complex was prepared from a mixture of $RuCl_3$ (0.1g, 1mmol), pyTz (0.14g, 2 mmol) and dicnq (0.13 g, 1mmol) in a manner analogous to that employed for the synthesis of *[Ru(dicnq)(pyTz)(phen)]BF_4* . Yield: 41%. m. p. >250 °C. Anal. Found: C, 49.245; H, 2.312; N, 33.202. Calcd. for RuC28H14N16: C, 49.255; H, 2.312; N, 33.289. ESI-MS: m/z 674.157, [M-2H]. IR (KBr, cm^{-1}): $\upsilon(C=N)_{pyTz}$ 1460, $\upsilon(N=N)_{pyTz}$ 1374, $\upsilon(C=N)_{py}$ 1616, $\upsilon(C\equiv N)_{dicnq}$=2223. ^{1}H NMR(DMSO-d6, 250 MHz): δ,9.51 (d, 1H), 9.43 (d, 1H), 8.52 (d, 2H), 8.31 (m, 2H), 8.11 (d, 2H), 7.76 (t, 2H), 7.46 (m, 4H).

2.3 Preparation of EL devices and testing

The structure of the fabricated device is as follow:

ITO/ PEDOT: PSS(55nm)/ PVK (60nm) /PBD (30nm)/Al (130nm) and, ITO/ PEDOT: PSS(55nm) / ruthenium complex (45nm) /Al (130 nm). PVK as a hole-transporting and PBD as an electron-transporting material were uesd. Glass substrates, coated with ITO (sheet resistance of 70 Ω/m^2), were used as the conducting anode PEDOT: PSS(poly(3,4-ethylenedi-oxythiophene): poly (styrenesulfonate)) was used as a hole injection and transporting layer. All polymeric layers were successively deposited onto the ITO coated-glass by using spin-coating process from the solution. A metallic cathode of Al was deposited on the emissive layer at 8×10^{-5} mbar by thermal evaporation. The PEDOT: PSS was dissolved in DMF, spin coated on ITO and was held in an oven at 120 °C for 2 hours after deposition. The optimized concentration of ruthenium complexes was fixed at 8% in the PVK: PBD host, whereas the Ru(dicnq) was varied from 6% to 14%. Subsequently, PVK, PBD and dicnq with weight ratio of 100,40, x (x=6 to 14) were separately dissolved in 8 mL of DMF, and then spin coated and baked at 80 °C for 1 hour. The thickness of the polymeric thin film was determined by a Dektak 8000. The EL intensity and spectra were measured with an ocean optic USB 2000, under ambient conditions. In addition, Keithley 2400 source meter was used to measure the electrical characteristics of the devices.

3. Results and Discussion

This part of the paper is divided into two sections. In section 3.1, we present the characterization data and photophysical properties of Ru(dicnq)(pyTz)(x),x=bpy, phen, bpy complexes. Section 3.2 examines the chemically modified compound, demonstrating that EL ~~color~~ can be tuned through ancillary ligand substitution.

3.1. Photophysical and electrochemical properties

The molecular structure of investigated complexes is shown in scheme 1. The absorption and emission spectra of complexes in DMF are displayed in Fig. 1. The dicnq, pyTz are largely responsible for the structured π – π * absorption bands between 200 and 350 nm [22]. The broad absorption band in the visible region is due to spin-allowed $d_\pi(Ru)\rightarrow\pi$ *(ligands) MLCT transition and overlapped transitions to different MLCT states, with the state, or degenerate states, at higher energy localized on the polypyridyl ligands [23].

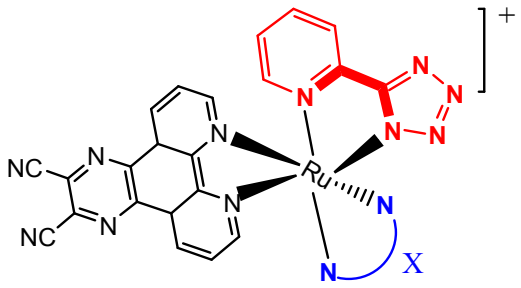

X= phen, bpy, pyTz

Scheme 1. Molecular structure of [Ru(dicnq)(pyTz)(X)] X=phen, bpy and pyTz

This effect of ancillary ligand is also reflected in the low energy metal to ligand charge transfer (MLCT) transitions where the λ_{max} of [Ru(dicnq)(*pyTz*)$_2$] is 481 nm and that of the [Ru(dicnq)(pyTz)(*bpy*)]BF_4 emitter is 462 nm. Surprisingly, the complex with phen moiety as ancillary ligand, [Ru(dicnq)(pyTz)(*phen*)], exhibited a blue shift in the lower energy MLCT band (440 nm) associated with an extinction coefficient of 14670 M^{-1} cm^{-1}.

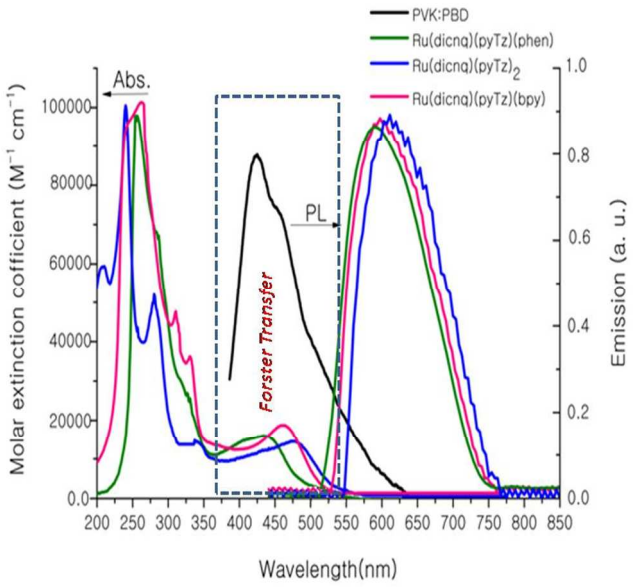

Figure 1. Right: absorption spectra of investigated complexes and left, PL spectra of PVK: PBD and complexes in DMF solvent 10^{-5} M. The emission spectra were recorded with 405 ± 2 nm excitation.

The PL spectra of ruthenium(II)–polypyridine complexes are largely attributed to the ^{3}MLCT states in the literature which are populated via an ultrafast ISC process from directly photoexcited ^{1}MLCT states [24-26]. As shown in Figure 1, the complexes emit yellowish-red light at room temperature with an emission maximum (l_{em}) at region 593-611 nm. Emission maxima, quantum yields and life time measurments are reported in Table 1. In this series, [Ru(dicnq)(pyTz)(bpy)]BF_4 has the highest quantum yield with Φ=0.01 in DMF solvent. In addition, all emission maxima are shifted to higher energies relative to $[Ru(phen)_3]^{2+}$, which is further indication of ancillary ligand substitution. Regarding the lifetime in Ru(dicnq)(pyTz)(X) complexes, it appears in the order bpy > phen> pyTz.

Table 1. EL and PL characteristics of Ru(dicnq) complexes.[a]: CIE=Commission Internationale deL'Eclairage; the ideal white is x= 0.33; y= 0.33.

	EL							PL		
Compound	EL_{max} [nm]	CIE[a] (x;y)	FWHM [nm]	Maximum current density, at 16 V	Turn-on V	Luminous efficiency [cd A^{-1}] at 16 V	Luminance [cd m^{-2}] at 16 V	PL_{max} [nm]	Φ [±0.001]	τ(ns) [±5]
Ru(dicnq)(pyTz)(phen)	521	0.34; 0.44	183	170	5.5	1.65	1020	593	0.008	330
Ru(dicnq)(pyTz)(bpy)	535	0.37; 0.43	179	117	5.2	1.78	1030	601	0.01	380
Ru(dicnq)$(pyTz)_2$	556	0.40; 0.39	197	66	6.3	0.87	865	611	0.005	245

The ^{1}H-NMR spectral data of complexes are consistent with conventional octahedral coordination geometries and diamagnetic behavior (t_{2g}^6) (see ESI†, S3a-c). In addition, the presence of dicnq of complexes are confirmed by FT-IR spectroscopy (ESI†, S4a-e). It is well established that the redox processes in Ru(II)-polypyridine complexes are mainly localized either on the metal center (oxidations) or on the ligands (reductions) [27, 28].

Cyclic voltammograms of the investigated Ru(dicnq) complexes are consistent with a metal-based reversible oxidation and several ligand-based reductions. It is, therefore, of fundamental importance to know the electrochemical behavior of the uncoordinated ligands to understand the pattern of the ligand-based redox series for the complexes. The half-wave potentials of ligand and Ru complexes are summarized in Table 2 (ESI†, S5). In acetonitrile containing 0.1 M $(TBA)BF_4$, dicnq and pyTz show a reversible one-electron-reduction wave at -0.66 V and two reversible for pyTz at -1.85 and -2.3 vs SCE. (Table 2). On the other hand, reduction of both dicnq ligands in $[Ru(phen)(dicnq)_2]^{2+}$ occurs below -1.0 V , followed by the reduction of phen or bpy in region -1.3 - -1.70 V and finally the reduction of pyTz ligand from -1.9 to -2.4 V. This means that the formal negative charge brought by the pyTz makes their reductions more difficult [29].

Thus, the relative ease of reduction of the ligands follows the order pyTz> phen/bpy> dicnq. It is useful to note the electron addition to dicnq ligands in $[Ru(dicnq)_3]^{2+}$ occurs at -0.47 V and oxidation of the ruthenium center occurs at +1.51 V, under similar experimental conditions of solvent and supporting electrolyte. On the other hand, a significant shift (around 300 mV) to higher negative potentials of the reduction process in [Ru(dicnq)pyTz] complexes compared to $[Ru(dicnq)_3]_2$ is observed upon ancillary ligand substitution of the complexes. In addition, the substitution of dicnq in $[Ru(dicnq)_3]^{2+}$ [21] with ancillary ligands decreases the oxidation potential of ruthenium steadily, resulting in an overall anodic shift of 200 mV for $[Ru(dicnq)(pyTz)]$ compared to $[Ru(dicnq)_3]^{2+}$. This trend is also seen in the known homolog ligands, when the dicnq in $[Ru(dicnq)_3]^{2+}$ replaces with phen ligand, the oxidations of the ruthenium center in $[Ru(phen)_2(dicnq)]^{2+}$, $[Ru(phen)(dicnq)_2]^{2+}$, and $[Ru(dicnq)_3]^{2+}$ occur at +1.31, +1.41, and +1.51 V, respectively [30] . Interestingly, the electron abstraction abilities from the metal center in Ru(dicnq)(pyTz)(x) (x=phen, bpy, pyTz) is very close to $[Ru(phen)_3]^{2+}$ (1.27 V). Whereas, the first reduction wave in Ru(dicnq)(pyTz) family is found to occur at less negative potentials than that of the $Ru(phen)_3]^{2+}$ (-1.35V) due to presence of dicnq ligand. These evidences confirm the key role of pyTz ligand as ancillary ligand to control the redox behavior of Ru polypyridyl complexes. In light of above observations, these data also suggests that the π* orbital of dicnq lies lower than that of ancillary ligands (phen/ bpy and pyTz) and, probably, that the added electron is delocalized equally on the π * levels of the dicnq ligands rather than on only one ligand [31]. As seen in table 2, the energy levels of HOMO and LUMO of investigated ruthenium complexes were calculated which are in agreement with DFT calculations (ESI†, S6a-c).

3. 2. EL properties

The structure of the fabricated device is as follow:

ITO/ PEDOT: PSS (55nm)/ PVK (60nm) /PBD (30nm)/ Al (130nm) and, ITO/ PEDOT: PSS (55nm)/ PVK (60nm)/ PBD (30nm)/ Ru(dicnq) complex (45nm) /Al (200nm), That is shown in Fig. 2. The EL spectra of the devices are shown in Fig 3. To analyze the energy transfer process from PVK to ruthenium complex and to find a relationship between the EL spectra of ruthenium compounds and PVK / PBD, an emissive layer without ruthenium complex was fabricated to record the PVK / PBD EL spectrum. It should be noted that high ratio of PBD leads to lower stability of the device due to the decrease in the ratio of PVK. 100:40 efficient ratio is suggested [32, 33], which reduces the risk of excimer formation and increases the stability of the device.

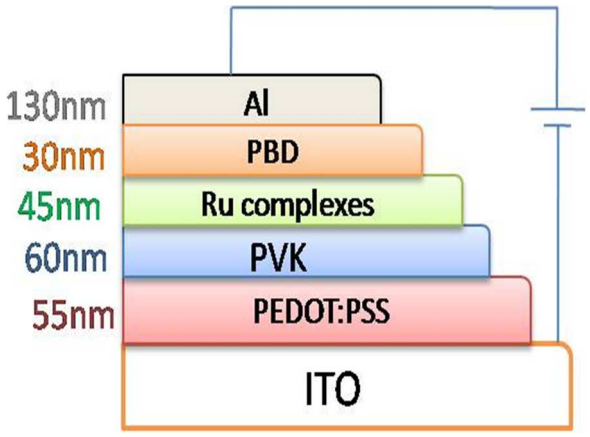

Figure 2. The layer arrangement of Ru(dicnq)-based LED.

As many reports and our analysis, the best concentration for PVK and PBD is 100 and 40, respectively. As shown in Fig. 4, the efficiency of the devices increases with increasing Ru(dicnq) concentration from 6 to 8 wt.%, but decreases when the dopant concentration is more than 8 wt. The device with 8 wt.% dopant has the highest luminance and current efficiency.

Table 2. Redox Potentials (mV) of ligands and Ru Complexes [a]

	E ½ (ox)	E ½ (red)					HOMO[b]	LUMO[b]	E_g(eV)
		(I)	(II)	(III)	(IV)	(V)			
		dicnq		phen/bpy		pyTz			
pyTz	-	-	-	-	-1.85	-2.3	-	-	-
dicnq	-	-0.65	-	-	-	-	-	-	-
(1)	+1.32	-1.08	-1.37	-	-1.90	-2.25	-5.72	3.32	2.40
(2)	+1.29	-0.97	-1.43	-1.70	-1.90	-2.23	-5.69	3.37	2.32
(3)	+1.30	-0.82	-	-	-1.93	-2.4	-5.70	3.58	2.05

[a]At room temperature and in MeCN solutions containing 0.1 M tetra-n-butyl ammonium tetrafloroborate. All $E_{1/2}$ values are referred to E ½ of the ferrocenium$^+$ /ferrocene redox couple (380 mV vs SCE in MeCN). [b] Energy levels estimated based on E_{ox} and E_{red}

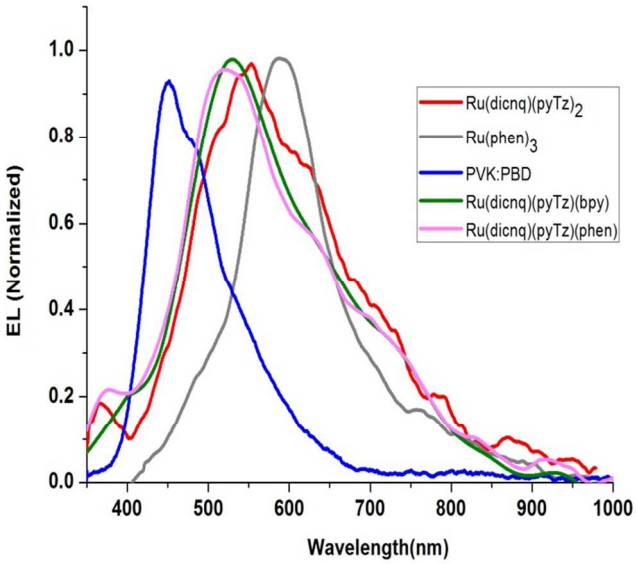

Figure 3. (a) EL spectra of PVK/PBD , $[Ru(phen)_3]^{2+}$ and Ru(dicnq)(pyTz)(X)]where X=bpy, phen and pyTz.

As shown in Fig. 3, the effect of ancillary ligand substitution on the spectral shift to a shorter wavelength induced a variation in the wavelength from 557 to 520 nm.

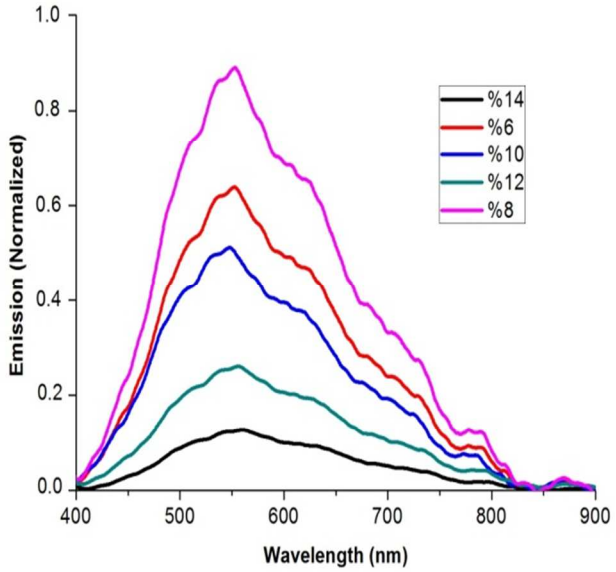

Figure 4: Influence of doping ratio on electroluminescence of $[Ru(dicnq)(pyTz)_2]$ at 16 V.

Interestingly, Ru(dicnq) complexes without pyTz ligand such as $[Ru(dicnq)_2(bpy)](BF_4)_2$, $[Ru(dicnq)_2(phen)](BF_4)_2$ and $[Ru(dicnq)_3](BF_4)_2$ were tested as emitter layers in the same LED cell, but the significance electroluminescence emission were not achieved. As an important result, the pyTz ligand has a key role to produce electroluminescence in Ru(dicnq) complexes. The basic characteristics and performance data are summarized in Table 2. As a general trend, the EL emission peak shifts to shorter wavelengths from $[Ru(dicnq)(pyTz)_2]$ through $[Ru(dicnq)(pyTz)(bpy)]BF_4$ to [Ru(dicnq)(pyTz)(phen)], correlating with the increase in the LUMO-HOMO energy gap 2.01, 2.2, and 2.27 eV for [Ru(dicnq)(pyTz)(*X*)] where X=pyTz, bpy and phen, respectively.

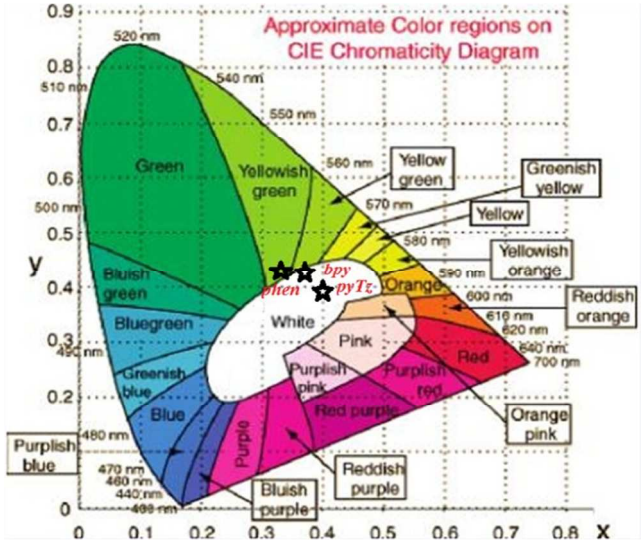

Figure 5. Plot of the CIE emission coordinates [34] of the [Ru(dicnq)(pyTz)(X)] where X=bpy, phen and pyTz .

At the same time, the EL characteristics of these devices are different. As CIE chromaticity diagram (Fig. 5), the emission from the device based on $[Ru(dicnq)(pyTz)(\textit{phen})]BF_4$ appeared to be close to a yellowish green hue; $[Ru(dicnq)(pyTz)(\textit{bpy})]BF_4$ had a yellow green hue, and $[Ru(dicnq)(pyTz)_2]$ had a white hue. It is useful to note, the perfect white light has CIE coordinates (0.33, 0.33). However, there is a quite broad region of the diagram around this point that can be considered white light [11b]. As shown in Fig. 6, a maximum luminance of 1020 cd/m^2 at 16 V was obtained from the device ITO/ PEDOT: PSS /PVK/ ruthenium complex/ PBD/ Al in which there was $[Ru(dicnq)(pyTz)(\textit{phen})]BF_4$ in emitting layer, however , the

luminance from the similar structure device in which [Ru(dicnq)(pyTz)(*bpy*)]BF_4 was used to increased to 1030 cd/m^2 at the same voltage. When [Ru(dicnq)(*pyTz*)$_2$] was used in the above device architecture the luminance was 865 cd/m^2 at 16V. Although the LED performance of this new class is not surprising compared to cyclometalated iridium complexes, this achievement is the good among the great of OLED performance in ruthenium polypyridyl complexes [35].

The schematic device architecture and the estimated energy-level diagram are depicted in Fig. 7. The observation and characterization of electroluminescence in this class of Ru(dicnq)(pyTz)(x), x=bpy , phen, pyTz emitter is of interest in the study of the fundamental electron transfer of this class of ruthenium polypyridyl-light emitting diodes. Here, the concept of Forster transfer in the energy transfer mechanism has been useful one. The PVK/ PBD/ Ru emitter pair has the appropriate spectral characteristics to act as a donor/acceptor pair in an energy transfer mechanism [36]. To be an effective means of energy transfer, the Forster mechanism has a number of conditions that must be satisfied, but two major considerations include the spatial separation between the donor and acceptor and the spectral characteristics of the donor emission and the acceptor absorption.

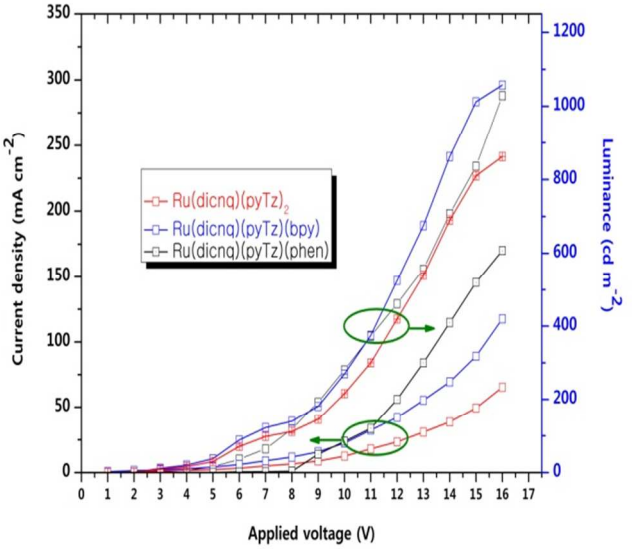

Figure 6. Current density and luminance versus applied voltage for Ru(dicnq)-devices

In addition, both modes of energy transfer require a level of spectral overlap of the donor emission and the acceptor absorption [37]. In this study, PVK has the spectral features to act as an energy transfer donor to Ru complexes by virtue of its 455 nm emission maxima, which overlaps the MLCT of Ru(dicnq) complexes. Moreover, the arrangement of layers has caused the Forster transfer of energy to result from PVK: PBD host to ruthenium complexes (ŏŏFig. 1).

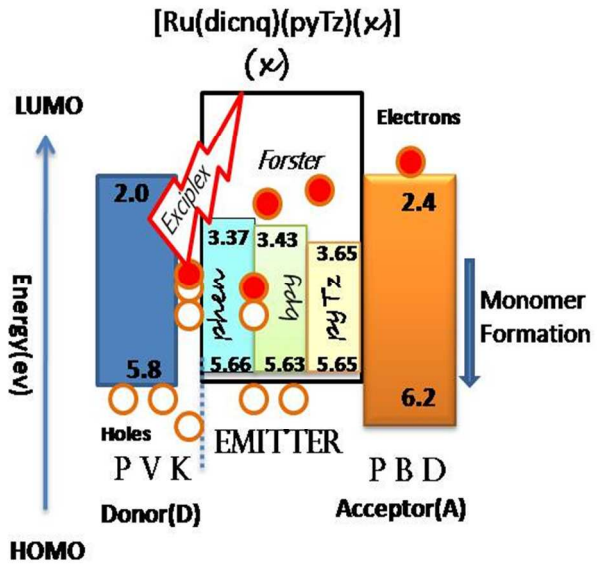

Figure 7. Schematic showing the energy levels of device and the dynamic process of emission. HOMO-LUMO level energy of the investigated emitters and other materials for LED device.

It should be noted that compared with the PL spectra, there is some red shift of the broad band in the EL one, which may be due to the different nature of EL- and PL-mechanisms. We suppose that the new broad band emission peaking at about 565 nm in EL spectrum of can likely be ascribed to the Exciplex under electrical excitation [38]. However, at the interface of two components in OLEDs, as reported in literatures [39], an Exciplex emission can occurs under both photoexcitation and electric fields. In this regard, the broadening and wavelength of PL spectrum of PVK/Ru(dicnq) film is also similar to EL spectrum that confirms an Exciplex transfer in the interface of PVK and Ru(dicnq) complexes (ESI. S7).

The new broad emission band at longer wavelength can originate from the intermolecular Exciplex. Generally, The Exciplex peaks shifted to a lower energy side in comparison to the peak related to the emitter layer because the emission energy of the Exciplex is smaller than that of the exciton in the EML [40]. The Exciplex emission can be explained from energy band theory, too. Electrons on the LUMO of PBD must overcome 0.3 eV potential barriers to inject onto LUMO of Ru(dicnq). Furthermore, the HOMO of PVK is very close to the HOMO of Ru(dicnq) , so the excited species will have a high probability to collide with PVK to form excited complex, [Ru(dicnq)$^-$ PVK$^+$]* which might result in the accumulation of holes at the PVK/ Ru(dicnq) interface [41]. When the voltage is increased, the electrons are injected into the PBD layer from Al cathode and the more holes recombine at the interface of the PVK: Ru(dicnq), which is result in the increasing of Exciplex emission (Fig. 8) [42].

The Exciplex formation and emission mechanisms under an applied electric field, including the generation of charge carriers, can be described by Scheme 2 and Fig. 7. In the scheme 2, Ru(dicnq)*(an excited state of Ru(dicnq)) forms an encounter complex (PVK$\cdots$ Ru(dicnq)*) in the presence of PVK (II), and then a radical ion pair (PVK$^+ \cdots$ Ru(dicnq) $^-$)* is produced by an intermolecular electron transfer from the PVK to Ru(dicnq)* [43].

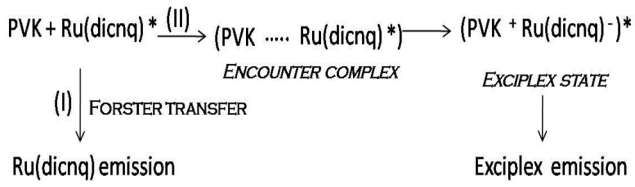

Scheme 2. Exciplex formation and emission mechanisms under applied electric field.

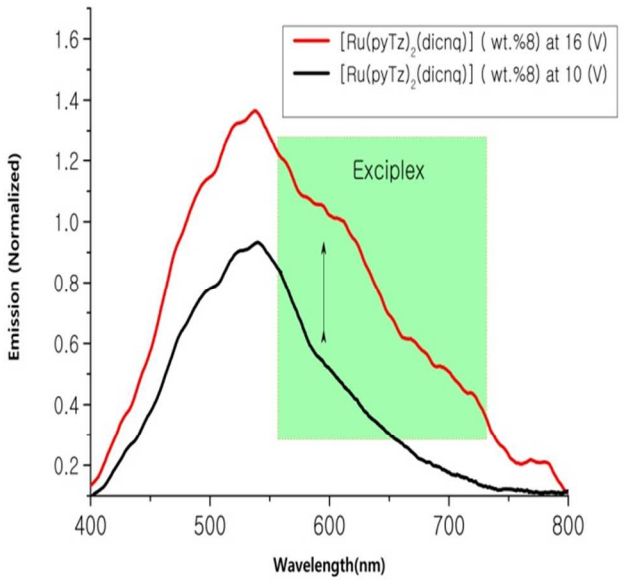

Figure 8: Influence of different applied voltages on electroluminescence of [Ru(dicnq)(pyTz)$_2$] at wt. %8.

Therefore, white light emission can be obtained from these multi-layer devices by combining Forster emission from Ru(dicnq) and Exciplex emission at PVK/ Ru(dicnq) interface, although the CIE chromaticity coordinates gradually change with applied voltages. The main challenge in ruthenium polypyridine chemistry lies in the ability to customize the net donating and acceptoring properties of the ancillary ligand(s) in order to modulate the Ru^{III} /Ru^{II} potential and the energy correlation between the emission energy and the HOMO–LUMO gap. The electron donor substitution on pyTz and/or dpq would be modified the tuning of photophysical properties, which can be followed in future works. Hereby, although the studied EL devices have not been fully optimized, their good performance characteristics give the basis to expect that the Ru(dicnq)(pyTz) complexes as luminescent materials would have a remarkable impact on the development of WOLEDs.

4. Conclusion

In this paper, the synthesis, characterization, photophysical and electrochemical properties of three new Ru(dicnq) complexes and their electroluminescence (EL) characteristics when employed as a dopant in ITO/ PEDOT: PSS/ PVK: PBD (100: 40: x% wt. Ru(dicnq)) /Al device are reported. We have successfully demonstrated an effective approach to produce white electroluminescence by adjusting the LUMO and HOMO levels of ruthenium complexes through the use of different ancillary ligand. We suggest that an Exciplex transfer occurred at the PVK–Ru complex interface when pyTz was incorporated as co-ligand into Ru(dicnq) complexes. We expected that the various fundamental properties elaborated in this study would be beneficial to the future development of Ru polypyridyl emitting materials for use as luminescent WOLEDs.

Acknowledgments:

The authors wish to thank the University of Zanjan for financial supports.

References

[1] (a)H. Xu, R. Chen, Q. Sun, W. Lai, Q.Su, W. Huang, X. Liu, *Chem. Soc. Rev*., 2014, **43**, 3259. (b) J. D. Slinker, J. Rivnay, J. S. Moskowitz, J. B. Parker, S. Bernhard, H. D. Abruña*a*, G. G. Malliaras, *J. Mater. Chem*., 2007, **17**, 2976.

[2] (a) V.W. Wah Yam, K. M-C. Wong, *Chem. Commun.*, 2011,**47**, 11579. (b) J. Bossert, C. Daniel, *Coord. Chem. Rev.* 2008, **254**, 2493.

[3](a) J. Jayabharathi, P. Ramanathan, V.Thanikachalam, *New, J. Chem.* 2015, DOI: 10.1039/C4NJ01515K. (b) M. Shang, C. Li, J. Lin, *Chem. Soc. Rev.*, 2014,**43**, 1372. (c) J. Morgado, F. Cacialli , R.H. Friend , R. Iqbal , G. Yahioglu ,L.R. Milgrom, S. C. Moratti , A. B. Holmes, *Chem. Phys. Lett.* 2000, **325**, 552.

[4] C. –X. Sheng, S. Singh, A Gambetta, T. Drori, M. Tong, S. Tretiak, and V. Vardeny;, *Sci. Rep.,* 2013, **3**, 2653.

[5] Q. Wang, D. Ma, *Chem. Soc. Rev.* , 2010, **39** , 2387.

[6]G. Schwartz, S. Reineke, T. C. Rosenow, K. Walzer and K. Leo, *Adv. Funct. Mater*., 2009, **19** , 1319.

[7] U. Giovannella, P. Betti, A. Bolognesi, S. Destri, M. Melucci, M. Pasini, W. Porzio and C. Botta, *Org. electron.*,2010, **11**, 2012.

[8] (a)G. M. Farinola and R. Ragni, *Chem. Soc. Rev.,* 2011, **40**, 3467., (b)Y. Takei, *Sci. Technol. Trends–Quarterly Rev*., 2009, **32** , 59.

[9] H. Shahroosvand, L. Najafi, E. Mohajerani, M. Janghouri, M. Nasrollahzadeh, *RSC Adv.* 2013, **4**, 1150.

[10] A. W. McKinleya, P. Lincoln , E. M. Tuite, *Coord. Chem. Rev.* 2011, **255**, 2676.

[11] A. J. McConnell, M. H. Lim, E. D. Olmon, H. Song, E. E. Dervan, J. K. Barton, *Inorg. Chem*. 2012, **51**, 12511. B. R. Spencer, B. J. Kraft, C. G. Hughes, M. Pink, J. M. Zalesk, *Inorg. Chem*. 2010, **49**, 11333,

[12] (a) S.-Y. Chang, J. Kavitha, S.-W. Li, C.-S. Hsu,Y. Chi,Y.-S. Yeh, P. –T. Chou, G.-H. Lee, A. J. Carty,Y.-T. Tao, C.-H. Chien, *Inorg. Chem*. 2006, **45**, 137. (b) C. Kasper , H. Alborzini , S. Can , I. Kitanovic , A. Meyer , Y. Geldmacher , M. Oleszak , I. Ott , S. Wölfl , W. S. Sheldrick, *J. Inorg. Biochemi*. 2012, **106**, 126.

[13] (a) A. P. Mosalkova, S.V. Voitekhovich, A. S. Lyakhov, L.S. Ivashkevich, J. Lach, B. Kersting, P. N. Gaponik, O. A. Ivashkevich, *Dalton Trans.*, 2013,**42**, 2985. (b) R. Hagen, J. G. Haasnoot, J. Reedijk, R. Wang, J. G. Vos, *Inorg. Chem*. 1991, **30**, 3263. (c) P. T. Chou, Y. Chi, *Chem. Eur. J*. 2007, **13**, 380.

[14] S.-J. Su, , C. Cai, , J. Takamatsu, , J. Kido, *Org. Electronics* 2012, **13**, 1937.

[15] Ilker Oner, Cigdem Sahin , Canan Varlikli, *Dyes. Pig*. 2012, **95**, 23.

[16] A. Garza-Ortiz, P. U. Maheswari, M. Siegler, A. L. Spek, J. Reedijk, *New J. Chem.*, 2013,**37**, 3450.

[17] (a) M. Thelakkat, H. Schmidt, *Adv. Mater*., 1998, **10**, 219,(b) S. Ashraf, M. Shahid, E. Klemm, M. Al-Ibrahim and S. Sensfuss, *Macromol. Rapid Commun*. , 2006, **27** , 1454.

[18] R. B. Nair, B. M. Cullum and C. J. Murphy, *Inorg. Chem*., 1997, **36**, 962.

[19] M. J. Frisch, G. W. Trucks, H. B. Schlegel, , G. E. Scuseria, M. A. Robb, J. R.Cheeseman, J. A. Montgomery, T. Vreven, K. N. Kudin, J. C. Burant, J. M. Millam, S. S. Iyengar, J. Tomasi, V. Barone, B. Mennucci, M. Cossi, G. Scalmani, N. Rega, , G. A. Petersson, H. Nakatsuji, M. Hada, M. Ehara, K. Toyota, R. Fukuda, J. Hasegawa, M. Ishida, T. Nakajima, Y. Honda, O. Kitao, H. Nakai, M. Klene, X. Li, J. E. Knox, H. P. Hratchian, J. B. Cross, V. Bakken, C. Adamo, J. Jaramillo, R. Gomperts, R. E. Stratmann, O. Yazyev, A. J. Austin, R. Cammi, C. Pomelli, J. W. Ochterski, P. Y. Ayala, K. Morokuma, G. A. Voth, P. Salvador, J. J. Dannen-berg, V. G. Zakrzewski, S. Dapprich, A. D. Daniels, M. C. Strain, O. Farkas, D. K. Malick, A. D. Rabuck, K. Raghavachari, J. B. Foresman, J. V. Ortiz, Q. Cui, A. G. Baboul, S. Clifford, J. Cioslowski, B. B. Stefanov, G. Liu, A. Liashenko, P. Piskorz, I. Komaromi, R. L. Martin, D. J. Fox, T. Keith, M. A. Al-Laham, C. Y. Peng, A. Nanayakkara, M. Challacombe, P. M. W. Gill, B. Johnson, W. Chen, M. W. Wong, C. Gonzalez, J. A.,Pople, Gaussian 03 Revision B.04, Gaussian Inc., Wallingford, *CT*, **2004**.

[20] (a) Z. Demko and K. Sharpless, *J. Org. Chem.,* 2001, **66**, 7945. (b) H. Shahroosvand, L. Najafi, A. Sousaraei, E. Mohajerani, M. Janghouri, *J. Mater. Chem. C*, 2013, **1**, 6970.

[21] A. Ambroise, B. G. Maiya, *Inorg. Chem.* 2000, **39**, 4264.

[22] (a) D. P. Rillema, D. G. Taghdiri, D. S. Jones, C. D. Keller, L. A. Worl, T. J. Meyer, H. A. Levy, *Inorg. Chem.* 1987, **26**, 578. (b) S. Bodige, A. S. Torres, D. J. Maloney, D. Tate, G. R. Kinsel, J. K. Walker, F. M. MacDonnell, *J. Am. Chem. Soc*. 1997, **119**, 10364.

[23] S. Delaney, M. Pascaly, P. K. Bhattacharya, K. Han, J. K. Barton, *Inorg. Chem.* 2002, **41**, 1966.

[24] D. Saha, S. Das, S. Mardanya, S. Baitalik, *Dalton Trans*. , 2012, **41**, 8886.

[25] P. I. P. Elliott, *Annu. Rep. Prog. Chem., Sect. A:Inorg. Chem*. , 2012,**108**, 389.

[26] M. J. Han, Y. M. Chen , K. Z. Wang, *New J. Chem.*, 2008, **32**, 970.

[27] H.J. Park, W. Kim, W. Choi, Y. K. Chung, *New J. Chem*., 2013,**37**, 3174.

[28] M. J. Fuentes, R. J. Bognanno, W. G. Dougherty, W.J. Boyko, W. S. Kassel, T. J. Dudley , J. J. Paul, *DaltonTrans*. , 2012, **41**, 12514.

[29] (a) S. Stagni, A. Palazzi, S. Zacchini, B. Ballarin, C. Bruno, M. Marcaccio, F. Paolucci, M. Monari, M. Carano, A. *J.* Bard, *Inorg. Chem.* 2006, **45**, 695. (b) S. Stagni, E. Orselli, A. Palazzi, L. De Cola, S. Zacchini, C. Femoni, M. Marcaccio, F. Paolucci, S. Zanarini, *Inog. Chem*, 2007*,* **46**, 9126.

[30] B. Gholamkhass, K. Koike, N. Negishi, H. Hori, K. Takeuchi, *Inorg. Chem.* 2001, **40,** 756.

[31] (a)Ackermann, M. N.; Interrante, L. V. *Inorg. Chem* .1984 , **23** , 3904. (b) Rillema, D. P.; Allen, G.; Meyer, T. J.; Conrad, D. *Inorg. Chem*., 1983 , **22** , 1617.

[32] J. Yang, K. Gordon, *Chem. Phys. Lett*. 2004, **385**, 481.

[33] S. Chang, C. Fan, C. Lai, Y. Chao, S. Hu, *Surf. Coat. Tech*. 2006, **200**, 3289

[34] B. Fortner, *Sci Tech J.*, 1996, **5**, 32.

[35] Y. Chuai , D-N Lee , C. Zhen , J-H. Min , B- H Kim , Dechun Zou, *Synt. Met*., 2004, **145**, 259.

[36] (a) V. Cleave, G. Yahioglu, P. Le Barny, R. H. Friend, N. Tessler, *Adv. Mater*., 1999, **11**, 285; (b) J. W. Yu, J. K. Kim, H. N. Cho, D. Y. Kim, C. Y. Kim, N. W. Song and D. Kim, *Macromolecules*, 2000, **33**, 5443.

[37] J. Kalinowski, *Opt. Mater*. 2008*,* **30***,* 792.

[38] Wen-Yi Hung, Guan-Cheng Fang, Yuh-Chia Chang, Ting-Yi Kuo, Pi-Tai Chou, Shih-Wei Lin, Ken-Tsung Wong, *ACS Appl. Mater. Interfaces* 2013, **5**, 6826.

[39] A. P. Kulkarni , S. A. Jenekhe, *J. Phys. Chem. C*., 2008, *112*, 5174.

[40] J. H. Yang , K. Gordon, B. H. Robinson, *Syn. Met*., 2003, **137**, 999.

[41] H. Yersin , A. F. Rausch, R. Czerwieniec, T. Hofbeck, T. Fischer , *Coord. Chem. Rev*., 2011, **255**, 2622.

[42] Y. Zhao, L. Duan, X. Zhang, D. Zhang, J. Qiao, G. Dong, L. Wang, Y. Qiu, *RSCAdv.* , 2013, **3**, 21453.

[43] N. Matsumoto, M. Nishiyama, C. Adachi, *J. Phys. Chem. C.,* 2008, **112**, 7735.